# Aeolian input of bioavailable iron to the ocean

Song-Miao Fan,[1] Walter J. Moxim,[1] and Hiram Levy II[1]

Received 21 October 2005; revised 22 February 2006; accepted 2 March 2006; published 7 April 2006.

[1] Atmospheric deposition of mineral dust supplies much of the essential nutrient iron to the ocean. Presumably only the readily soluble fraction is available for biological uptake. Previous ocean models assumed this fraction was constant. Here the variable solubility of Fe in aerosols and precipitation is parameterized with a two-step mechanism, the development of a sulfate coating followed by the dissolution of iron (hydr)oxide on the dust aerosols. The predicted soluble Fe fraction increases with transport time from the source region and with the corresponding decrease in dust concentration. The soluble fraction is ~1 percent near sources, but often 10–40 percent farther away producing a significant increase in soluble Fe deposition in remote ocean regions. Our results may require more rapid biological and physicochemical scavenging of Fe than used in current ocean models. We further suggest that increasing $SO_2$ emission alone could have caused significant Fe fertilization in the modern northern hemisphere oceans. **Citation:** Fan, S.-M., W. J. Moxim, and H. Levy II (2006), Aeolian input of bioavailable iron to the ocean, *Geophys. Res. Lett.*, *33*, L07602, doi:10.1029/2005GL024852.

## 1. Introduction

[2] Marine phytoplankton growth is influenced by dissolved iron in seawater [e.g., *Sunda and Huntsman*, 1997]. Nitrogen fixation and cycling by marine organisms are also found to depend on the concentration of dissolved Fe [*Falkowski*, 1997]. Atmospheric transport and deposition of dust particles originating from deserts supplies much of the Fe that sustains biological production in the ocean. The solubility of Fe in dust is thus an important parameter in the global iron connections between desert dust, ocean biogeochemistry, and climate [*Jickells et al.*, 2005].

[3] Current global ocean biogeochemical models assume constant Fe solubilities between 1–10% when specifying bioavailable Fe fluxes from simulated aeolian dust deposition [e.g., *Gregg et al.*, 2003; *Moore et al.*, 2004]. However, available measurements of Fe solubility in aerosols and precipitation (see Table 1) indicate high variability and a much wider range. Furthermore, since high Fe solubility has often been measured at low dust concentrations [*Chen and Siefert*, 2004; *Baker et al.*, 2006] and dust concentrations decrease with distance of transport, Fe solubility would appear to increase with particle age in the atmosphere. For example, in Table 1 African dust samples contain soluble Fe ranging from 6% at Barbados to 26% on the east coast of North America and from 10% in the Mediterranean to 17% farther north in France. Realistic modeling of atmospheric deposition of bioavailable Fe must adequately represent this observed geographical variability of Fe solubility.

[4] Noting that measured Fe solubility is small near the deserts where dry deposition dominates, and is larger downwind where wet deposition dominates, *Gao et al.* [2003] estimated aeolian Fe input to the ocean using a solubility range of 1–6% for dry deposition and 10–50% for wet deposition. Hematite ($\alpha$-$Fe_2O_3$) is the main form of mineral Fe in dust originating from the deserts. Hematite dissolution is very slow at the pH typical of rainwater (3.5–5.5), and is promoted by protons at low pH (<2) [*Meskhidze et al.*, 2003]. Here we use a global atmospheric model to calculate the soluble fraction of Fe in dry and wet deposition. Unlike *Luo et al.* [2005], who examined various processes influencing iron solubility with a single kinetic rate that, in the case of sulfate, depended on local sulfate concentrations, we explicitly use a two-step mechanism, the conversion of dust from fresh to acid coated that depends on local $SO_2$ concentrations, followed by the formation of dissolved phases that does not (see auxiliary material[1]).

## 2. Methods

[5] The Geophysical Fluid Dynamics Laboratory global chemical transport model (GCTM) driven by NCEP reanalysis is used for this study [*Fan et al.*, 2004]. The model has 28 vertical (sigma) levels, equal-area horizontal grids with 265 km resolution, and modules for mineral dust entrainment and deposition. We assume newly entrained dust particles are hydrophobic and are subsequently converted to hydrophilic by gas uptake or cloud processing (see below). Hydrophobic particles are removed by ice nucleation and raindrop impaction scavenging; while hydrophilic particles are also removed by droplet nucleation.

[6] Three types of dust/iron tracer are carried in the GCTM to separate the three life stages for dust particles: fresh, coated, and dissolved (for Fe). The mass of each type is distributed in four size bins (0.2–2, 2–3.6, 3.6–6, and 6–12 $\mu$m in diameter). Within each size bin, particle mass is transferred from fresh to coated, and from coated to dissolved, as a first-order kinetic process.

[7] The rate coefficient to convert dust particles from fresh to coated by heterogeneous reactions is calculated from $k_N[HNO_3] + k_S[SO_2]$ ($s^{-1}$), where $k_N = 0$ at RH < 25%, increasing linearly to $k_N = 5 \times 10^{-6}$ $ppb^{-1}s^{-1}$ at RH $\geq$ 35%, $k_S = 0$ at RH < 50%, increasing linearly to $k_S = 3 \times 10^{-6}$ $ppb^{-1}s^{-1}$ at RH $\geq$ 60%, and the gas concentrations are given in ppbv. With large uncertainties in the reaction rates, these values are chosen to obtain agreement

[1]Geophysical Fluid Dynamics Laboratory, NOAA, Princeton, New Jersey, USA.



[1]Auxiliary material is available at ftp://ftp.agu.org/apend/gl/2005gl024852.

**Table 1.** Measurements of Dust Fe Solubility in Aerosols and Precipitation Defined as the Ratio of Dissolved Fe Passing Through 0.4 μm Pore Size Filters, to Total Fe Concentration in a Sample and Model Results[a]

| Location | Date | Number of Samples | Soluble Fe (Obs, Model), % | References[b] |
|---|---|---|---|---|
| | | *Rain and Snow* | | |
| NE Mediterranean (Turkey) | Feb 1996–Jun 1997 | 87 | 10, 12 | 1 |
| NW Mediterranean (Tour du Valat) | 1988–1989 | 45 | 11, 9 | 2 |
| Britanny, France | Sep and Nov | 6 | 17, 22 | 3 |
| Rhode Island, USA | Apr, May and Jul | 8 | 17, 36 | 4 |
| North Carolina, USA | Jul 1997–Jun 1999 | 81 | 26, 31 | 5 |
| Antarctica | Aug–Dec | 31 | 32, 20 | 6 |
| Summit, Greenland | Ice core | 17 | 40, 39 | 7 |
| Bermuda Island | Mar and Aug | 12 | 68, 30 | 8 |
| | | *Aerosols* | | |
| Atlantic cruise, 26°N | Jan–Feb 2001 | 7 | 32, 22 | A |
| Atlantic cruise, 15°N | Jan–Feb 2001 | 23 | 5, 5 | B |
| Atlantic cruise, 5°N | Jul–Aug 2001 | 24 | 5, 5 | C |
| Atlantic cruise, 15°N | Jul–Aug 2001 | 6 | 3, 6 | D |
| Pacific cruise | Apr 2001 | 18 | 2, 22 | E |
| Pacific Islands | Jan–Oct | 27 | 56, 27 | F |
| Atlantic cruise (49°N–25°N) | Sep 2001,Oct 2002 | 17 | 12 (2–54), 20 (4–49) | G |
| Atlantic cruise (21°N–6°N) | Oct 2000, Sep 2001 | 6 | 8 (2–25), 7 (3–16) | H |
| Barbados (13°N) | Sep and Oct | 25 | 6, 4 | I |
| Atlantic cruise (1°N–11°S) | Oct 2000, Oct 2001 | 10 | 10 (4–24), 21 (13–34) | J |
| Atlantic cruise (16°S–42°S) | Oct 2001 | 9 | 9 (4–17), 12 (1–22) | K |

[a]Note 1–2% of particulate Fe may pass through. As examples of variability, range of solubility is given in parenthesis for each of the *Baker et al.* [2006] data.

[b]1, *Ozsoy and Saydam* [2001]; 2, *Guieu et al.* [1997]; 3, *Colin et al.* [1990]; 4, *Zhuang et al.* [1992]; 5, *Kieber et al.* [2001]; 6, *Edwards and Sedwick* [2001]; 7, *Laj et al.* [1997]; 8, *Kieber et al.* [2003]; A–D, *Chen and Siefert* [2004]; E, *Hand et al.* [2004]; F, *Zhuang et al.* [1992], G,H,J,K, *Baker et al.* [2006]; I, *Zhu et al.* [1997]. The letters and numbers are used to label data points in Figure 1.

between the model and observed trends of dust concentration from Izania to Barbados, and farther to Miami and Bermuda [*Fan et al.*, 2004], with the relative magnitude of $k_N$ and $k_S$ based on laboratory measurements [*Underwood et al.*, 2001; *Usher et al.*, 2002].

[8] We also consider cloud processing in the transfer of mass from fresh to coated: cloud droplets collect dust particles and gaseous $SO_2$ followed by aqueous oxidation of $SO_2$ and droplet evaporation in non-precipitating events [*Levin et al.*, 1996]. Particle scavenging by droplet impaction is based on the cross-section of a spherical particle colliding with a droplet due to the difference in their terminal velocities and on measured collection efficiencies [*Kerkweg et al.*, 2003]. The rate of cloud processing is proportional to cloud volume fraction ($f_{cld}$) in a model grid box that is diagnosed from relative humidity. Here, dependence on $SO_2$ concentration is neglected. A constant number density of 200 $cm^{-3}$ and a radius of 10 μm are assumed for the droplets in all non-precipitating clouds. In this simplified treatment an e-folding time for fresh particles of 30 days is obtained at $f_{cld} = 0.2$.

[9] The rate of dust mass transfer from coated to dissolved is the rate of Fe dissolution normalized by a factor of 0.035 (the average mass fraction of hematite Fe in dust). The production of dissolved Fe from hematite is calculated from $R_{Fe} = R_d AnM/w$, where $R_{Fe}$ is grams of Fe dissolved per gram of hematite Fe per second, $R_d$ is the dissolution rate in a unit surface area, A is the specific surface area of hematite, n = 2 (moles Fe/mole hematite), M is (55.8 g $mol^{-1}$), and w is the mass fraction of Fe in hematite [*Meskhidze et al.*, 2003]. A wide range of dissolution rates have been measured for iron (hydr)oxide at low pH (<2) and in the presence of light and ligand ($R_d = 10^{-11}$–$10^{-10}$ mol hematite $m^{-2}$ $s^{-1}$) [*Duckworth and Martin*, 2001; *Martin*, 2005]. We use $R_d = 4 \times 10^{-11}$ mol $m^{-2}$ $s^{-1}$ and $A = 100$ $m^2$ $g^{-1}$ to obtain a good global agreement between model and measured Fe solubility. These values correspond to an e-folding time of 18 days for dissolution. Much slower dissolution rates have been assumed previously [*Meskhidze et al.*, 2003; *Hand et al.*, 2004]. The solubility is calculated as the fraction of iron (hydr)oxides that has dissolved in the aqueous shell, and has a lower limit of 0.5% [*Zhuang et al.*, 1992].

## 3. Results

[10] Table 2 shows the global total input of dust and soluble Fe to the ocean calculated in this study. Global deposition of 592 Tg/yr is within the range of previous model results [*Mahowald et al.*, 2005]. Wet deposition accounts for 80% and dry deposition 20% of the total soluble Fe input to the ocean, compared to the even partitioning for mineral dust deposition. The mass weighted global average Fe solubility is 17% for wet deposition, and is 4.6% for dry deposition. The solubility for total deposition is 11%, close to the upper limit (10%) assumed in current ocean biogeochemistry models, however, we find that the geographic range of Fe solubility is quite large.

**Table 2.** Global Atmospheric Deposition Fluxes of Dust and Fe to the Ocean as Calculated in the Model[a]

| | Wet Deposition | Dry Deposition | Total Deposition |
|---|---|---|---|
| Mineral dust, Tg/yr | 312 | 280 | 592 |
| Extractable Fe, Tg/yr | 11 | 10 | 21 |
| Soluble Fe, Tg/yr | 1.8 | 0.45 | 2.3 |
| Average solubility, % | 17 | 4.6 | 11 |

[a]1994–1998 average; 1 Tg = $10^{12}$ g.

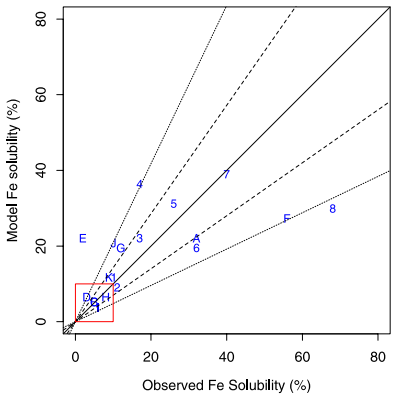


**Figure 1.** Model and observed Fe solubility. Numerals are for precipitation, and letters are for aerosol. Locations are shown in Table 1. Model results are averaged over five years (1994–1998) at the long-term stations and for the days and corresponding grid-box locations along the cruises. The red box encloses the solubility range of 1%–10% commonly assumed in current ocean models. The black solid line indicates a 1:1 relation. The dashed and dotted lines show 25% and 50% departures from the 1:1 relation, respectively.

[11] Figure 1 compares model results and measurements and shows good qualitative agreement, with 17 data points scattered close to the 1:1 line, only 2 data points are outside the 50% distance lines. Fe solubility ranges from 2% to 40%, and is frequently much larger than the upper limit of 10% used in ocean models [e.g., *Fung et al.*, 2000]. The model thus captures the observed increase of Fe solubility with distance from dust source regions (see Table 1). The September–October data from Barbados and the *Baker et al.* [2006] cruises provide a unique latitudinal transect of the Atlantic ocean, crossing through a region of climatologically high dust concentration north of the ITCZ originating from the Sahara. Both measurements and model show relatively high solubility north of 25°N; lowest values associated with the high dust concentrations (21°N–6°N); and higher solubilities south of the equator decreasing again south of 16°S.

[12] Our soluble Fe fluxes, in comparison with those calculated assuming a constant Fe solubility of 5%, are shown in Figure 2. The positive difference in fluxes is largest around India, downwind of East Asia and Sahel, while the negative difference is largest downwind of Sahara and Patagonia sources (Figure 2c). The absolute flux difference is larger in the Northern Hemisphere than in the Southern Hemisphere, due to more rapid chemical processing by air pollution in the former, and is small in the Southern Ocean. However, the largest relative differences (Figure 2d) are found in the more remote regions of the central Pacific, Arctic and subarctic, and Indian oceans, reflecting the older age and increased chemical dissolution of Fe since emission.

## 4. Discussion

[13] In general, our model predicts small Fe solubility and large dust deposition near the sources and large Fe solubility corresponding to smaller dust deposition distant from source regions. The distribution of soluble Fe deposition from this study is thus more uniform than estimates with an assumed constant solubility. This has immediate implications to Fe cycling in the ocean, for which we have very limited measurements. Present ocean models have all adapted to Fe fluxes based on constant solubility and neglected the potential impact of air pollution. Our results suggest that anthropogenic emissions of $SO_2$ and NO should have caused a significant increase in hematite dissolution and soluble Fe input to the North Atlantic and North Pacific Oceans since the industrial revolution. The impact of this un-intended Fe fertilization of the ocean could have been large, and is a subject for future research.

[14] Globally, our model deposition of 2.3 Tg/yr of soluble Fe can support a primary production of 50 PgC/yr in the ocean if we assume a cellular Fe:C ratio of 10 μmol/mol and neglect removal by abiotic scavenging. The cellular Fe:C ratios are found to increase with Fe availability, ranging from 5–50 μmol/mol for dissolved Fe between 0.01–0.6 nM [*Sunda and Huntsman*, 1997]. The global primary productivity predicted by ocean models is on the order of 50 PgC/yr [e.g., *Moore et al.*, 2004], and the global particulate export is estimated at 10 PgC/yr from the surface to the deep ocean [*Gnanadesikan et al.*, 2002]. These values indicate that, unlike the major nutrients, re-mineralization of organic matter in the mixed layer does not lead to significant iron recycling.

[15] Regionally, our model indicates atmospheric deposition of bioavailable Fe between 100–200 μmol $m^{-2}yr^{-1}$

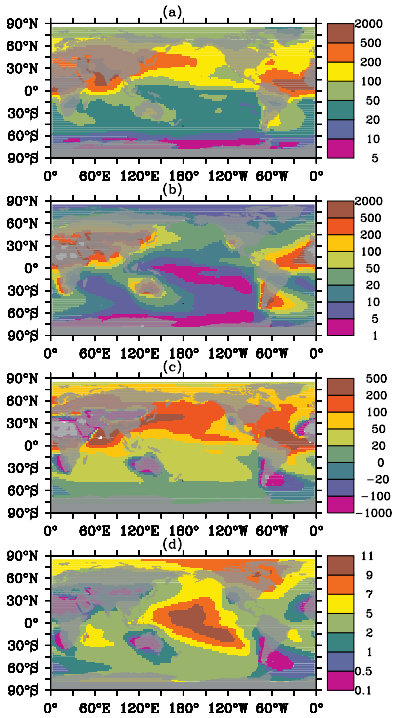


**Figure 2.** (a) Annual deposition fluxes (μmol $m^{-2}$ $yr^{-1}$) of dissolved Fe to the ocean based on our 2-step solubility process. (b) Annual deposition fluxes of dissolved Fe to the ocean based on a constant 5% solubility. (c) Difference of fluxes shown in Figures 2a and 2b. (d) Ratio of fluxes shown in Figures 2a and 2b.

in the subarctic Pacific, which can result in 1–2 nM dissolved Fe in a 100 m column in a year. In comparison, the annual Fe assimilation has been previously estimated at 77 μmol $m^{-2}yr^{-1}$ using an Fe:C ratio of 4.5 (mol/mol for the region [*Fung et al.*, 2000], which would be 170 μmol $m^{-2}yr^{-1}$ for an Fe:C ratio of 10 μmol/mol. The observed concentration of dissolved Fe in the region is about 0.2 nM on the average [*Gregg et al.*, 2003]. For our model calculated Fe deposition, the residence time of Fe in the surface ocean is estimated to be 0.1–0.2 years at steady state, which is smaller than the modeled mean residence time of 1.3 years based a smaller dust Fe solubility (2%) [*Moore et al.*, 2004]. This large difference in residence time suggests that the ocean models may have under-estimated biological assimilation of Fe and scavenging by mineral dust particles.

[16] **Acknowledgments.** We thank Alex Baker for providing the Atlantic cruise data and Larry Horowitz for providing the model $SO_2$ fields. We are grateful to John Dunne, Paul Ginoux, Anand Gnanadesikan, and Jorge Sarmiento for comments on the original draft, and to Natalie Mahowald and an anonymous reviewer for very useful suggestions on the final manuscript.

## References

Baker, A. R., T. D. Jickells, M. Witt, and K. L. Linge (2006), Trends in the solubility of iron, aluminium, manganese and phosphorus in aerosol collected over the Atlantic Ocean, *Mar. Chem.*, *98*, 43–58.

Chen, Y., and R. L. Siefert (2004), Seasonal and spatial distribution and dry deposition fluxes of atmospheric total and labile iron over the tropical and subtropical North Atlantic Ocean, *J. Geophys. Res.*, *109*, D09305, doi:10.1029/2003JD003958.

Colin, J. L., J. L. Jaffrezo, and J. M. Gros (1990), Solubility of major species in precipitation: Factors of variation, *Atmos. Environ., Part A*, *24*(3), 537–544.

Duckworth, O. W., and S. T. Martin (2001), Surface complexation and dissolution of hematite by $C_1$–$C_6$ dicarboxylic acids at pH = 5.0, *Geochim. Cosmochim. Acta*, *65*(23), 4289–4301.

Edwards, R., and P. Sedwick (2001), Iron in East Antarctic snow: Implications for atmospheric iron deposition and algal production in Antarctic waters, *Geophys. Res. Lett.*, *28*(20), 3907–3910.

Falkowski, P. G. (1997), Evolution of the nitrogen cycle and its influence on the biological sequestration of $CO_2$ in the ocean, *Nature*, *387*, 272–275.

Fan, S.-M., L. W. Horowitz, H. Levy II, and W. J. Moxim (2004), Impact of air pollution on wet deposition of mineral dust aerosols, *Geophys. Res. Lett.*, *31*, L02104, doi:10.1029/2003GL018501.

Fung, I. Y., S. K. Meyn, I. Tegen, S. C. Doney, J. G. John, and J. K. B. Bishop (2000), Iron supply and demand in the upper ocean, *Global Biogeochem. Cycles*, *14*(1), 281–295.

Gao, Y., S.-M. Fan, and J. L. Sarmiento (2003), Aeolian iron input to the ocean through precipitation scavenging: A modeling perspective and its implication for natural iron fertilization in the ocean, *J. Geophys. Res.*, *108*(D7), 4221, doi:10.1029/2002JD002420.

Gnanadesikan, A., R. D. Slater, N. Gruber, and J. L. Sarmiento (2002), Oceanic vertical exchange and new production: A comparison between models and observations, *Deep Sea Res., Part II*, *49*, 363–401.

Gregg, W. W., P. Ginoux, P. S. Schopf, and N. W. Casey (2003), Phytoplankton and iron: Validation of a global three-dimensional ocean biogeochemical model, *Deep Sea Res., Part II*, *50*, 3143–3169.

Guieu, C., et al. (1997), Atmospheric input of dissolved and particulate metals to the northwestern Mediterranean, *Deep Sea Res., Part II*, *44*, 655–674.

Hand, J. L., N. M. Mahowald, Y. Chen, R. L. Siefert, C. Luo, A. Subramaniam, and I. Fung (2004), Estimates of atmospheric-processed soluble iron from observations and a global mineral aerosol model: Biogeochemical implications, *J. Geophys. Res.*, *109*, D17205, doi:10.1029/2004JD004574.

Jickells, T. D., et al. (2005), Global iron connections between desert dust, ocean biogeochemistry, and climate, *Science*, *308*, 67–71.

Kerkweg, A., S. Wurzler, T. Eisin, and A. Bott (2003), On the cloud processing of aerosol particles: An entraining air-parcel model with two-dimensional spectral cloud microphysics and a new formulation of the collection kernel, *Q. J. R. Meteorol. Soc.*, *129*, 1–18.

Kieber, R. J., K. Williams, J. D. Willey, S. Skrabal, and G. B. Avery Jr. (2001), Iron speciation in coastal rainwater: Concentration and deposition to seawater, *Mar. Chem.*, *73*, 83–95.

Kieber, R. J., J. D. Willey, and G. B. Avery Jr. (2003), Temporal variability of rainwater iron speciation at the Bermuda Atlantic Time Series Station, *J. Geophys. Res.*, *108*(C8), 3277, doi:10.1029/2001JC001031.

Laj, P., et al. (1997), Distribution of Ca, Fe, K, and S between soluble and insoluble material in the Greenland Ice Core Project ice core, *J. Geophys. Res.*, *102*(C12), 26,615–26,623.

Levin, Z., E. Ganor, and V. Gladstein (1996), The effects of desert particles coated with sulfate on rain formation in the eastern Mediterranean, *J. Appl. Meteorol.*, *35*, 1511–1523.

Luo, C., N. Mahowald, N. Meskhidze, Y. Chen, R. L. Siefert, A. R. Baker, and A. Johansen (2005), Estimation of iron solubility from observations and a global aerosol model, *J. Geophys. Res.*, *110*, D23307, doi:10.1029/2005JD006059.

Mahowald, N., et al. (2005), The atmospheric global dust cycle and iron inputs to the ocean, *Global Biogeochem. Cycles*, *19*, GB4030, doi:10.1029/2005GB002541.

Martin, S. T. (2005), Precipitation and dissolution of iron and manganese oxides, in *Environmental Catalysis*, edited by V. H. Grassian, pp. 61–81, CRC Press, Boca Raton, Fla.

Meskhidze, N., W. L. Chameides, A. Nenes, and G. Chen (2003), Iron mobilization in mineral dust: Can anthropogenic $SO_2$ emissions affect ocean productivity?, *Geophys. Res. Lett.*, *30*(21), 2085, doi:10.1029/2003GL018035.

Moore, J. K., S. C. Doney, and K. Lindsay (2004), Upper ocean ecosystem dynamics and iron cycling in a global three-dimensional model, *Global Biogeochem. Cycles*, *18*, GB4028, doi:10.1029/2004GB002220.

Ozsoy, T., and A. C. Saydam (2001), Iron speciation in precipitation in the north-eastern Mediterranean and its relationship with Sahara dust, *J. Atmos. Chem.*, *40*, 41–76.

Sunda, W. G., and S. A. Huntsman (1997), Interrelated influence of iron, light and cell size on marine phytoplankton growth, *Nature*, *390*, 389–392.

Underwood, G. M., C. H. Song, M. Phadnis, G. R. Carmichael, and V. H. Grassian (2001), Heterogeneous reactions of $NO_2$ and $HNO_3$ on oxides and mineral dust: A combined laboratory and modeling study, *J. Geophys. Res.*, *106*(D16), 18,055–18,066.

Usher, C. R., A. Al-Hosney, S. Carlos-Cuellar, and V. H. Grassian (2002), A laboratory study of the heterogeneous uptake and oxidation of sulfur dioxide on mineral dust particles, *J. Geophys. Res.*, *107*(D23), 4713, doi:10.1029/2002JD002051.

Zhu, X. R., J. M. Prospero, and F. J. Millero (1997), Diel variability of soluble Fe (II) and soluble total Fe in North African dust in the trade winds at Barbados, *J. Geophys. Res.*, *102*(D17), 21,297–21,305.

Zhuang, G., Z. Yi, R. A. Duce, and P. R. Brown (1992), Chemistry of iron in marine aerosols, *Global Biogeochem. Cycles*, *6*(2), 161–173.

S.-M. Fan, H. Levy II, and W. J. Moxim, Geophysical Fluid Dynamics Laboratory, NOAA, Princeton, NJ 08544-308, USA. (Songmiao.Fan@noaa.gov)